Direct modulation and optical confinement factor modulation of semiconductor lasers

A. Frommer, S. Luryi,[a] D. T. Nichols, J. Lopata, and W. S. Hobson
AT&T Bell Laboratories, Murray Hill, New Jersey 07974

(Received 24 April 1995; accepted for publication 10 July 1995)

A method for modulation of semiconductor lasers based on the modulation of the optical confinement factor is demonstrated. Using this method, an enhanced -3 dB bandwidth is observed in agreement with the small signal rate equation analysis. A modulation response that drops at high frequencies slower than the conventional direct current modulation response is achieved. © *1995 American Institute of Physics.*

Semiconductor lasers are critically important elements in optical communications systems. An essential requirement is a high modulation bandwidth with reduced driving currents. The conventional method of directly modulating the driving current, has a bandwidth which at low and moderate currents is limited by the $1/f^2$ decay of the modulation response above the relaxation oscillation frequency.[1] Recently Gorfinkel and co-workers[2–6] have discussed theoretically laser modulation by controlling other laser parameters such as the optical gain or optical confinement factor. A laser structure suitable for an optical confinement factor modulation scheme has been proposed.[5,6] In this letter we report the experimental comparison of the direct modulation response and the optical confinement factor modulation response. The -3 dB bandwidth of the latter is shown to be almost twice as large as that of the former. The low frequency response of the laser is in good agreement with the small signal analysis of the rate equations, when the role of electrical parasitics is taken into account. At high frequencies a decreased decay rate of the optical confinement factor modulation response is observed as compared to that of the direct modulation response. This is attributed to the theoretical $1/f$ intrinsic response drop of the former as compared to the $1/f^2$ intrinsic decay for the latter.

The laser structure studied is shown in Fig. 1. We fabricated ridge-waveguide $In_{0.2}Ga_{0.8}As/GaAs$ single quantum well lasers grown in a vertical geometry MOCVD reactor.[7] The layers were grown on a (100) n^+ GaAs substrate and consist of the following layers: a 0.5 μm GaAs buffer layer, a 0.1 μm undoped GaAs optical confinement layer, an 80 Å $In_{0.2}Ga_{0.8}As$ quantum well, a 0.1 μm undoped GaAs optical confinement layer, a 1.2 μm p^- InGaP cladding layer, and a 0.2 μm p^+ GaAs cap layer. Three parallel ridges were defined using wet chemical etching. A central 6 μm wide ridge waveguide and two additional 20 μm wide ridges on both its sides were formed. They were separated by two 5 μm chemically etched grooves. The grooves are 1.3 μm deep, and etched off the p^+ GaAs cap layer and 1.1 μm out of the 1.2 μm p^- InGaP cladding layer. The three ridges are connected to three Au pads using two metallization layers with a dielectric in between. The central pad is connected to the central ridge, and the two side pads make contact to the two side ridges. A detailed picture of the various metal and dielectric layers is shown in Fig. 1. The wafer was then cleaved into laser chips with 500 μm cavity length.

For device operation, the driving current is applied between the top center electrode and the substrate contact. When an additional modulating signal is applied between these terminals driving current modulation is achieved. The two side electrodes connecting the side ridges are used for the modulation of the laser optical confinement factor. For optical confinement factor modulation, a dc current source between the top central ridge and the substrate maintains a constant current flow through the device. When the voltage applied to the side contacts provides additional forward bias to the areas below the side ridges additional current will flow in these regions. The result is an additional spreading of the driving current into these regions.[5,6] When the voltage applied to the side contacts is of the opposite polarity, the voltage drop along the *PN* junction under the side contacts is decreased, therefore less current will flow in these regions. The driving current will thus be confined to flow mainly under the central ridge-waveguide stripe. The lateral optical mode profile is determined only by the ridge-waveguide ge-

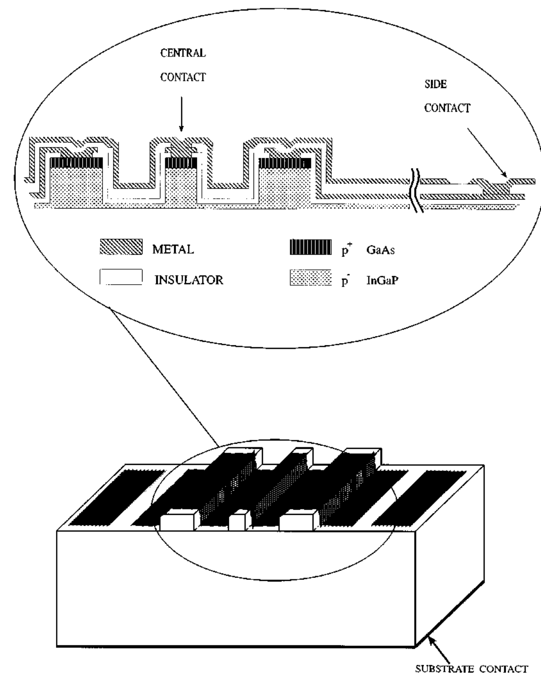

FIG. 1. Structure of the $In_{0.2}Ga_{0.8}As/GaAs$ single quantum well ridge waveguide laser with additional side contacts for lateral carrier distribution control.

[a]Currently at the State University of New York at Stony Brook, Stony Brook, NY 11794.

Downloaded¬13¬Dec¬2001¬to¬129.49.69.110.¬Redistribution¬subject¬to¬AIP¬license¬or¬copyright,¬see¬http://ojps.aip.org/aplo/aplcr.jsp

ometry and is fixed. Lasing takes place in the areas where population inversion is maintained. The current lateral distribution affects the width of this active region. Thus, by controlling the current lateral distribution the side voltages control the lateral confinement factor Γ. Simultaneously, the side voltages affect also the average current density in the active area J.[6] Applying a modulating signal to the side contacts while maintaining a constant dc current through the device will thus result in a dual J and Γ modulation action. Near field radiation patterns of the laser below threshold as well as $L-I$ characteristics measurements where performed under different bias conditions of the side contacts. These measurements showed similar results to those observed by Gorfinkel *et al.*,[5,6] and support the dual J and Γ modulation action of the side contacts. Electrical simulations of carrier lateral distribution below threshold (no stimulated emission), using the device simulator PADRE,[8] confirm the action of the side potentials on the carrier redistribution.

The small signal solution to the rate equations gives the laser's intrinsic frequency response for direct current modulation as:

$$R_J=\frac{f_0^2}{[(f^2-f_0^2)^2+f^2(\gamma/2\pi)^2]^{1/2}}. \tag{1}$$

f is the modulating frequency, f_0 is the resonant frequency, and γ is the damping rate. Small signal analysis of the rate equations for Γ modulation gives a laser frequency response of the form:[4–6]

$$R_\Gamma=\frac{f_0^2(1+f^2\tau_0^2)^{1/2}}{[(f^2-f_0^2)^2+f^2(\gamma/2\pi)^2]^{1/2}}, \tag{2}$$

where τ_0 is a characteristic time describing the efficiency of the optical confinement factor modulation. τ_0 depends on the photon density, and decreases with increasing pumping current.[6] Equation (2) can be shown to apply also for the case of simultaneous modulation of J and Γ, as is the case in our laser structure.[6] Only the value of γ_0 in Eq. (2) is different between the case of pure Γ modulation and the case of dual J and Γ modulation. We will thus refer from now to modulation applied to the side contacts as to Γ modulation.

The small signal frequency response of the laser was measured for both direct J modulation and for Γ modulation using an HP8703A lightwave component analyzer. Figures 2 and 3 show the small signal frequency responses of the laser for the two schemes of modulation. The curves are considerably different from each other as predicted by Eqs. (1) and (2). The resonance peak is enhanced for the Γ modulation case due to the term $f^2\tau_0^2$ in the numerator. It is also observed that the Γ modulation response has a -3 dB bandwidth almost twice as large as that of the J modulation response.

In order to compare the experimental data to the theory, the role of the electrical parasitics in determining the modulation response of the laser must be taken into account.[1,9,10] A low frequency RC rolloff is caused by the oxide capacitance and series resistance. We utilize the commonly used expression:[10]

$$R_e=\frac{1}{[1+(f/f_{RC})^2]^{1/2}} \tag{3}$$

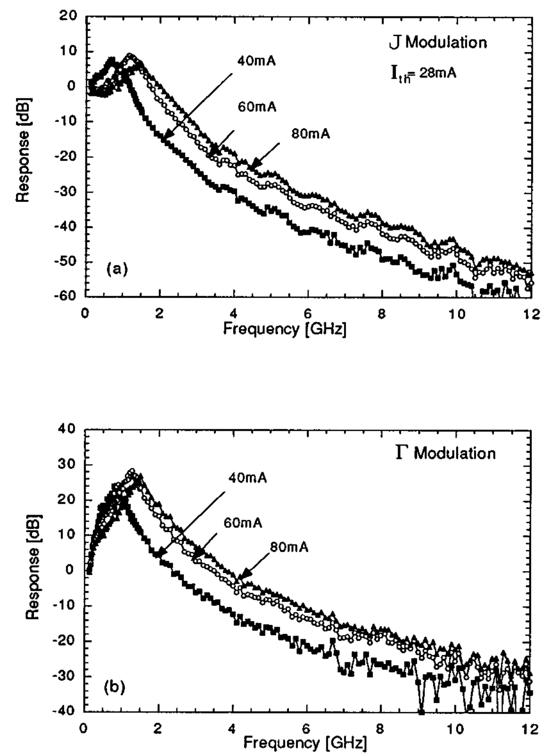

FIG. 2. (a) Small signal J modulation response at various bias currents (b). Small signal Γ modulation response for same bias currents as in (a).

to describe the low frequency RC rolloff of the laser. Taking into account only Eq. (3) for the electrical response of the laser, we expect a good fit to the experimental data for low frequencies. At higher frequencies additional parasitics become important. We assume that up to 4 GHz the only parasitics contributing to the response is the RC rolloff described by Eq. (3). The full laser modulation response up to 4 GHz is thus approximated by:

$$\begin{aligned} R&=R_J R_e \quad \text{for } J \text{ modulation,}\\ R&=R_\Gamma R_e \quad \text{for } \Gamma \text{ modulation.}\end{aligned} \tag{4}$$

At each bias point, the response in the low frequency range ($f<4$ GHz) is analyzed by performing a fit of Eq. (4) to the measured curves. The fit determines the parameters f_0, γ, τ_0, and f_{RC}. For a given bias f_0 and γ are the same for the J and for the Γ modulation. The Γ modulation response, however, has a much lower parasitic rolloff frequency f_{RC}. From the fits we determine $f_{RC}^\Gamma\approx 0.85$ GHz, whereas $f_{RC}^J\approx 3.6$ GHz. This is expected, since our laser structure implies a much higher RC limitation for the side contacts since they are connected with a long and wide first metallization layer. This metallization layer is the major component of the parasitic capacitance in our structure. This type of contact layer is not needed in the case of the central electrode, therefore the direct modulation scheme has a much higher f_{RC}. Figure 3(a) shows a typical example of the fits obtained. A good fit is obtained for the low frequency range. The different behavior of the J and Γ modulation responses is well predicted by Eq. (4). Using the parameters fitted to the experimental results, Fig. 3(a) shows also the deduced intrinsic response of the laser for the J and Γ modulation schemes, R_J and R_Γ, respectively. The laser's intrinsic Γ modulation response is shown to have a -3 dB bandwidth

Downloaded¬13¬Dec¬2001¬to¬129.49.69.110.¬Redistribution¬subject¬to¬AIP¬license¬or¬copyright,¬see¬http://ojps.aip.org/aplo/aplcr.jsp

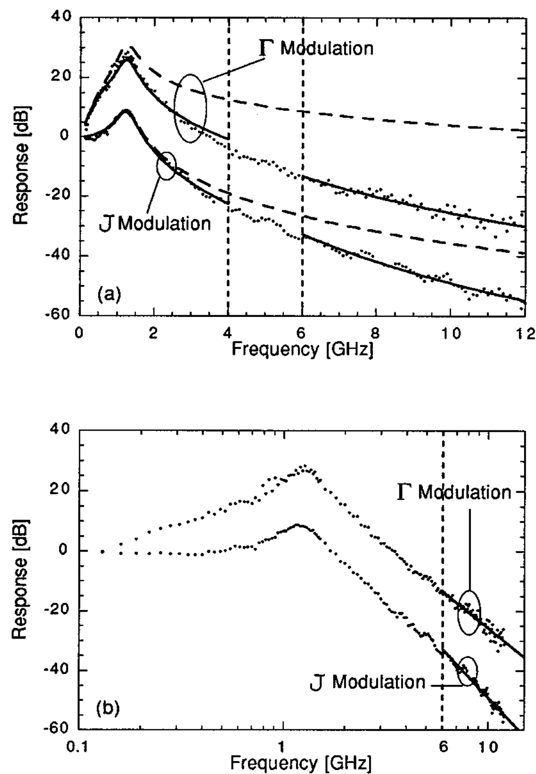

FIG. 3. (a) J and Γ modulation responses for $I_{\mathrm{pump}}=60$ mA. The solid lines are fits to the low frequency range, $f<4$ GHz [Eq. (4)], and to the high frequency range, $f>6$ GHz [Eq. (5)]. The dashed lines are the laser's intrinsic responses extracted from the fitted parameters. (b) Same as (a) but in logarithmic scale. The solid lines are the fits to the high frequency range, showing the different decay rates of the modulation response for the J and Γ modulation schemes.

higher than 20 GHz as compared to ~2 GHz for the direct J modulation.

For frequencies well above the resonant frequency, $f>f_0,\ 1/\tau_0$, Eqs. (1) and (2) predict an intrinsic $1/f$ decay of the response for the Γ modulation as compared to a $1/f^2$ drop of the direct J modulation response. At high frequencies, however, the additional rolloff caused by the diffusion capacitance becomes important[10] and other electrical parasitic elements might also contribute to the overall electrical response decay rate. Recently, transport across the separate confinement heterostructure (SCH) was shown to introduce a rolloff of the modulation response, with a break frequency given by $\sim 1/2\pi\tau_s$, where τ is the carrier transport time across the SCH.[11] For our laser structure with SCH of 2000 Å, $\tau_s \sim 30$ ps.[11] This corresponds to a carrier transport rolloff frequency of ~5 GHz. Thus, Eq. (4) does not fully account for the electrical and carrier transport response terms which become important for $f \geqslant 5$ GHz. In order to compare the high frequency response of the two modulation schemes, we suggest a phenomenological description of the laser response at high frequencies as:

$$R_{\mathrm{hf}} \propto \frac{1}{f^n}, \tag{5}$$

where n is a fitting parameter, including the overall intrinsic and parasitic response of the laser at high frequencies. We perform a least squares fit of Eq. (5) to the experimental data for the high frequency range which is taken to be $f>6$ GHz. A good fit is obtained for the different bias conditions. A typical example is shown in Fig. 3, where $n_J \approx 3.7$ and $n_\Gamma \approx 2.8$. For all bias points the Γ modulation response gives a high frequency decay rate smaller than that of the J modulation response, and the difference $n_J - n_\Gamma$ varies between 0.7 and 0.9 for the different bias conditions. It is not unity, however, as would be predicted due to the difference in the intrinsic behaviors alone. This is attributed to the different electrical responses for the two cases. The rf modulation signal applied to the side contacts suffers both, from the electrical parasitics experienced by the direct modulation rf signal, and from the series resistance and the additional capacitances which are related to the metal layers connecting the side electrodes in our structure. It is thus expected that the Γ modulation electrical (parasitic) response will have a steeper decay. This partially masks out the pure intrinsic behavior in the experimental data. However, for all bias conditions $n_J - n_\Gamma \geqslant 0.7$ due to the $1/f$ intrinsic behavior of the Γ modulation as compared to the $1/f^2$ intrinsic behavior of the conventional J modulation.

In conclusion, we have demonstrated experimentally the Γ modulation of a laser diode. The enhanced resonance peak predicted by the small signal analysis of the rate equations is clearly observed in the measurements, and the low frequency behavior of the response is in good accord with the theory. At high frequencies a smaller decay rate of the Γ modulation response as compared to J modulation is observed. The lower decay rate is due to the intrinsic smaller decay rate of the Γ modulation response. Additional parasitics, however, complicate the analysis. Our results show that a higher modulation bandwidth is achieved with the Γ modulation scheme, and suggest that in a structure, optimized for high speed operation, a very high modulation bandwidth can be achieved with low driving currents. In such a structure, the parasitic rolloff frequency (such as f_{RC} or $1/2\pi\tau_s$) is made high. For low driving currents f_0 is small and the modulation bandwidth for J modulation is limited to $\sim f_0$, due to the $1/f^2$ intrinsic rolloff of the response above f_0. In contrast, the Γ modulation response will be limited only by the parasitic rolloff even at low driving currents, since it drops only as $1/f$ above f_0. It can thus have a high modulation bandwidth with much reduced driving currents.

[1] K. Y. Lau and A. Yariv, Semicond. Semimet. **22B**, 70 (1985).
[2] V. B. Gorfinkel and S. Luryi, Appl. Phys. Lett. **60**, 3141 (1992).
[3] V. B. Gorfinkel and S. Luryi, Appl. Phys. Lett. **62**, 2923 (1993).
[4] E. A. Avrutin, V. B. Gorfinkel, S. Luryi, and K. A. Shore, Appl. Phys. Lett. **63**, 2460 (1993).
[5] V. B. Gorfinkel, G. Kompa, M. Novotny, S. A. Gurevich, G. E. Shtengel, and I. E. Chebunina, IEDM Tech. Digest (**1993**), 933
[6] V. B. Gorfinkel, S. A. Gurevich, I. E. Chebunina, M. S. Shatalov, and G. E. Shtengel (unpublished).
[7] W. S. Hobson, T. D. Harris, C. R. Abernathy, and S. J. Peterson, Appl. Phys. Lett. **58**, 77 (1991).
[8] M. R. Pinto, D. M. Boulin, C. S. Rafferty, R. K. Smith, W. M. Coughran, I. C. Kizilyalli, and M. J. Thoma, IEDM Tech. Digest (**1992**) 923.
[9] J. E. Bowers, Solid State Electron. **30**, 1 (1987).
[10] R. Olshansky, P. Hill, V. Lanzisera, and W. Powazinik, IEEE J. Quantum Electron. **QE-23**, 1410 (1987).
[11] R. Nagarajan, T. Fukushima, M. Ishikawa, J. E. Bowers, R. S. Geels, and L. A. Coldren, IEEE Photonics Technol. Lett. **4**, 121 (1992), and references therein.

Downloaded¬13¬Dec¬2001¬to¬129.49.69.110.¬Redistribution¬subject¬to¬AIP¬license¬or¬copyright,¬see¬http://ojps.aip.org/aplo/aplcr.jsp